Journal Pre-proof

Bile acid-terpyridine conjugates: Steroidal skeleton controlled AIE effect and metal-tunable fluorescence and supramolecular assembly properties

Chao Liu, Kaiyu Zhang, Qinxing Sun, Weina Li

PII: S0040-4020(20)30432-4

DOI: https://doi.org/10.1016/j.tet.2020.131283

Reference: TET 131283

To appear in: *Tetrahedron*

Received Date: 17 December 2019

Revised Date: 10 May 2020

Accepted Date: 12 May 2020

Please cite this article as: Liu C, Zhang K, Sun Q, Li W, Bile acid-terpyridine conjugates: Steroidal skeleton controlled AIE effect and metal-tunable fluorescence and supramolecular assembly properties, *Tetrahedron* (2020), doi: https://doi.org/10.1016/j.tet.2020.131283.

Graphical Abstract

To create your abstract, type over the instructions in the template box below.
Fonts or abstract dimensions should not be changed or altered.

Bile acid-terpyridine conjugates: steroidal skeleton controlled AIE effect and metal-tunable fluorescence and supramolecular assembly properties

Leave this area blank for abstract info.

Chao Liu†[ab], Kaiyu Zhang†[a], Qinxing Sun[a] and Weina Li[a,*]

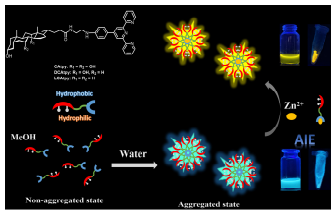

Journal Pre-proof

Tetrahedron

journal homepage: www.elsevier.com

Bile acid-terpyridine conjugates: steroidal skeleton controlled AIE effect and metal-tunable fluorescence and supramolecular assembly properties

Chao Liu†[ab], Kaiyu Zhang†[a], Qinxing Sun[a] and Weina Li [a, *]

[a] College of Chemistry and Pharmaceutical Sciences, Qingdao Agricultural University, Qingdao, 266109, China.
[b] School of Materials Science and Technology, China University of Geosciences (Beijing), Beijing, 100083, China
† These authors contributed equally to this article

ARTICLE INFO

Article history:
Received
Received in revised form
Accepted
Available online

Keywords:
Bile acid
Terpyridine
Conjugates
AIE
Tunable fluorescence

ABSTRACT

Herein, a series of conjugates combining bile acid and terpyridine units were developed. Based on the unique rigid skeleton and excellent amphiphilicity of bile acid fragment, the aggregation properties of three conjugates are finely regulated and the resulted aggregates can strongly confine and tune the rotation of terpyridine units to endow the three conjugates with excellent different AIE properties. Furthermore, with the excellent metal coordination properties, terpyridine units endow the conjugates with excellent metal response properties and lead to various colourful complexes. The supramolecular assembly morphology can also be well controlled by the metal ions. These biological conjugates with controllable AIE properties and metal tunable fluorescence and supramolecular assembly properties may provide a new avenue for the bioimaging and drug controllable delivery system.

1. Introduction

Organic luminescent materials have attracted significant attention due to their potential applications in optical recording,[1, 2] lighting equipment,[3-6] bioimaging,[7-9] sensors[10] and so forth. However, weakening or quenching of the fluorescence emission always occurs in their concentrated solutions or during the formation of films, which is referred to as aggregation-caused quenching (ACQ) effect and limits the usage of traditional luminescent materials.[11] In 2001,[12] Tang and co-workers firstly reported the aggregation-induced emission (AIE) phenomenon that is opposite to ACQ. With the enhanced luminescence emission and quantum yields in the solid state or in the aggregate form, much effort has been devoted to develop AIE luminogens. And a series of archetypal AIE luminogens, such as hexaphenylsilole (HPS),[13] tetraphenylethylene (TPE),[14] biphenyl,[15] tetraphenylpyrazine (TPP)[16] and tetraphenyl-1,4-butadiene (TPBD),[17] arylbenzene, arylethene[18] etc. have been explored. Terpyridine (tpy) and its derivatives are well-investigated ligands for transition metal ions and can produce highly stable complexes with fascinating optical, electronic, and magnetic properties.[19-22] Recently, terpyridine-Zn^{2+} complexes exhibiting efficient intramolecular charge transfer have been explored as novel metal based AIE active luminogen.[23-26] Tian and coworkers exhibited that the bare organic terpyridine can also act as AIE active luminogen.[27] The AIE properties of terpyridine and its derivatives are attracting increasing interest from various research fields.[28-31]

Bile acids are a class of natural occurring compounds with unique concave rigid skeleton, fascinating facial amphiphilicity, and excellent biological compatibility.[32] By combining with bile acid skeleton, a series of functional chemical systems, such as adaptable foldamers,[33-35] supramolecular assemblies,[36-43] shape-memory polymers,[44] elastomer-like materials,[45] molecular necklace,[46] and superchiral coordination complexes[47] have been constructed. And bile acid skeleton exhibited excellent structure controllable and tunable abilities.

In this paper, a series of conjugates combing bile acid and terpyridine units were developed. It is demonstrated that the two fragments can retain their respective properties well and endow the conjugates with new properties. The three conjugates CAtpy, DCAtpy, and LCAtpy (Scheme 1) exhibit similar optical properties in different solvents, such

* Corresponding author. Tel.: +0-532-8608-0894; fax: +0-532-8608-0213; e-mail: wnli@qau.edu.cn

as MeOH, CH_2Cl_2, THF, and DMF. While the solvent polarity can affect the position and intensity of their fluorescence emission peak. For example, the fluorescence emission of the three compounds is quenched in MeOH and shows strong emission at about 450 nm in THF. This phenomenon might be attributed to twisted intramolecular charge transfer (TICT) state with a strong dependence on the solvent polarity. Because of bile acid fragment possessing the unique rigid skeleton and excellent amphiphilicity, the aggregation properties of three conjugates are finely regulated and the resulted aggregates can strongly confine and tune the rotation of terpyridine units to endow the conjugates excellent AIE properties. Furthermore, with the excellent metal coordination properties, terpyridine units endow the conjugates with excellent metal response properties, thus leading to various colourful complexes. And the supramolecular assembly morphology can also be well controlled by the metal ions. These biological conjugates with controllable AIE properties and metal tunable fluorescence and supramolecular assembly properties may provide a new avenue for the bioimaging and drug controllable delivery system.

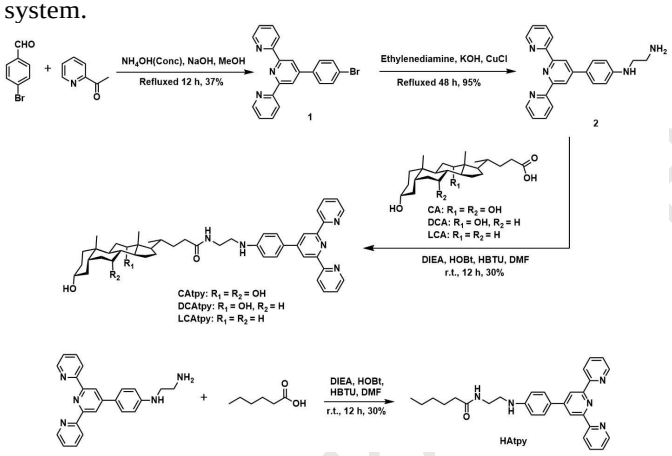

Scheme 1. Synthetic routes of CAtpy, DCAtpy, LCAtpy and HAtpy.

2. Experimental

2.1 General information

All the chemicals were used as received without further purification unless were specifically stated. 4-Bromobenzaldehyde, 2-acetylpyridine, hexanoic acid (HA), N-Hydroxybenzotriazole (HOBt), N,N-diisopropylethylamine (DIEA), O-benzotriazole-N,N,N',N'-tetramethyl-uronium-hexafluorophosphate (HBTU), cuprous chloride and metal ions were purchased from Energy Chemical Technology Co. Ltd. (Shanghai). The cuprous chloride was washed with acetic acid and ethyl ether until the solid turned white. Cholic acid (CA), deoxycholic acid (DCA), and lithocholic acid (LCA) were purchased from Aladdin Industrial Corporation. All the solvents (analytically pure) were obtained from Sinopharm Chemical Reagent Company. Column chromatography was performed with Aluminium oxide neutral (200-300 mesh FCP) with the solvent mixtures specified in the corresponding experiment.

^{1}H and ^{13}C NMR were recorded on a BRUKER AVANCE III HD 500 MHz spectrometer (Central Laboratory of QAU). Electrospray ionization mass spectrometry (ESI-MS) was measured on a Bruker ESQUIRE-LC spectrometer in positive or negative mode. High-resolution electrospray ionization mass spectrometry (HRMS) was measured using quadrupole time-of-flight (Q-TOF) as mass analyzer. The UV-Vis absorption spectra were recorded on a Hitachi U-3900 Spectrophotometer (Tokyo, Japan) using 10 mm path length quartz cuvettes. The fluorescence measurements were performed using F-2700 FL Spectrophotometer (Tokyo, Japan) and the mission slit width was kept at 10 nm. Transmission electron microscopy (TEM) images were collected on an HT7700 transmission electron microscope (Central Laboratory of QAU). The dynamic diameters of aggregates were measured by dynamic light scattering (DLS) using Zetasizer Nano ZSE system (Malvern).

2.2 Synthesis of 4'-(4-bromophenyl)-2,2':6',2''-terpyridine (compound 1)

To a 120 mL MeOH solution of 4-bromobenzaldehyde (1000 mg, 5.40 mmol) was added 2-acetylpyridine (1310 mg, 10.80 mmol), NaOH (220 mg, 5.40 mmol), and 30 mL concentrated NH_4OH (aq.). The reaction mixture was refluxed for 12 h. The oil-bath was then removed, and the reaction mixture was cooled to room temperature. The slight yellow precipitate was filtered and washed sequentially with deionized H_2O and MeOH. The precipitate collected from the filtration was purified by column chromatography with aluminium oxide neutral (CH_2Cl_2:MeOH = 1:1) to give target product as white powder. Yield: 37%. ^{1}H NMR (500 MHz, $CDCl_3$): δ = 8.73 (d, J = 5.0 Hz, 2H, terpyridine 3, 3"-H), 8.70 (s, 2H, terpyridine 3', 5'-H), 8.67 (d, J = 8.0 Hz, 2H, terpyridine 6, 6"-H), 7.86-7.90 (t×d, J_1 = 8.0 Hz, J_2 = 1.5 Hz, 2H, terpyridine 4, 4"-H), 7.78 (d, J = 8.5 Hz, 2H, bromophenyl H), 7.64 (d, J = 8.5 Hz, 2H, bromophenyl H), 7.35-7.37 (t×d, J_1 = 5.0 Hz, J_2 = 1.5 Hz, 2H, terpyridine 5, 5"-H). ^{13}C NMR (125 MHz, $CDCl_3$): δ = 156.05, 156.01, 149.12, 149.01, 137.36, 136.92, 132.09, 128.87, 123.94, 123.47, 121.39, 118.53. HRMS (ESI), m/z calcd for $[C_{21}H_{14}BrN_3+H]^+$ = 388.0449, 390.0429, found 388.0436, 390.0426.

2.3 Synthesis of 4'-(4-N-aminoethylene phenyl)-2,2':6',2''-terpyridine (compound 2)

To ethylenediamine (0.2 mL, 3 mmol) solution of 4'-(4-bromophenyl)-2,2':6',2"-terpyridine (388 mg, 1 mmol) was added KOH (112 mg, 2 mmol) and CuCl (40 mg, 0.1 mmol) under N_2 atmosphere. Then the reaction tube was sealed and the mixture was refluxed for 48 h, during which the colour of solution turned yellow. The refluxed solution was cooled to room temperature. Afterwards, water was added and the yellow solid was obtained, which was filtered under reduced pressure and purified by column chromatography with aluminium oxide neutral (CH_2Cl_2:MeOH = 10:1) to give

target product. Yield: 95%. ^{1}H NMR (500 MHz, $CDCl_3$): δ = 8.73 (d, J = 4.0 Hz, 2H, terpyridine 3, 3"-H), 8.69 (s, 2H, terpyridine 3', 5'-H), 8.66 (d, J = 8.0 Hz, 2H, terpyridine 6, 6"-H), 7.87 (t, J = 8.0 Hz, 2H, terpyridine 4, 4"-H), 7.82 (d, J = 8.0 Hz, 2H, phenyl H), 7.34 (t, J = 6.0 Hz, 2H, terpyridine 5, 5"-H), 6.75 (d, J = 7.5 Hz, 2H, phenyl H), 4.32 (br, 1H, phenyl-*NH*), 3.28 (m, 2H, phenyl-NH-CH_2), 3.01 (t, J = 6.0 Hz, 2H, CH_2-NH_2), 1.56 (br, 2H, NH_2). ^{13}C NMR (125 MHz, $CDCl_3$): δ = 156.64, 155.71, 150.03, 149.37, 149.08, 136.81, 128.33, 126.80, 123.65, 121.37, 117.57, 112.99, 46.25, 41.13. HRMS (ESI), m/z calcd for $[C_{23}H_{21}N_5\text{-}H]^-$ = 366.1718, found 366.1724.

2.4 Synthesis of bile acid-terpyridine conjugates and the reference compound

Compound 2 (367 mg, 1 mmol) and bile acid or hexanoic acid (1 mmol), were added into the solution of HOBT (135 mg, 1 mmol), HBTU (379 mg, 1 mmol) and DIEA (192 mg, 1 mmol) in DMF (10 mL). The mixture was stirred at room temperature for 12 h. Then water was added and yellow solid was obtained, which was filtered under reduced pressure and purified by column chromatography with aluminium oxide neutral (CH_2Cl_2:MeOH = 20:1) to give target product as yellow solid. Yield: 30%.

Cholic acid-terpyridine conjugate (CAtpy): ^{1}H NMR (500 MHz, $CDCl_3$): δ = 8.72 (d, J = 4.0 Hz, 2H, terpyridine 3, 3"-H), 8.66 (s, 2H, terpyridine 3', 5'-H), 8.64 (d, J = 8.0 Hz, 2H, terpyridine 6, 6"-H), 7.85-7.89 (m, 2H, terpyridine 4, 4"-H), 7.81 (d, J = 8.5 Hz, 2H, phenyl H), 7.33-7.36 (m, 2H, terpyridine 5, 5"-H), 6.72 (d, J = 9.0 Hz, 2H, phenyl H), 3.91 (br, 1H, 12β-CH), 3.74 (br, 1H, 7β-CH), 3.54 (m, 2H, phenyl-NH-CH_2), 3.43 (br, 1H, 3β-CH), 3.36 (m, 2H, CH_2-NH), 0.95-2.35 (m, 24H, steroidal skeleton and alkyl H), 0.92 (d, J = 6.0 Hz, 3H, 21-CH_3), 0.82 (s, 3H, 19-CH_3), 0.60 (s, 3H, 18-CH_3). ^{13}C NMR (125 MHz, $CDCl_3$): δ = 175.38, 156.58, 155.60, 150.07, 149.48, 149.00, 136.98, 128.32, 126.21, 123.75, 121.54, 117.52, 112.74, 73.13, 71.95, 68.33, 46.30, 45.88, 43.99, 41.67, 41.50, 39.69, 39.34, 39.05, 35.34, 35.04, 34.72, 32.34, 31.48, 30.57, 28.16, 27.55, 26.39, 23.25, 22.39, 17.45, 12.39. HRMS (ESI), m/z calcd for $[C_{47}H_{59}N_5O_4\text{+H}]^+$ = 758.4645, found 758.4640.

Deoxycholic acid-terpyridine conjugate (DCAtpy): ^{1}H NMR (500 MHz, CD_3OD): δ = 8.70 (d, J = 4.0 Hz, 2H, terpyridine 3, 3"-H), 8.65 (d, J = 8.0 Hz, 2H, terpyridine 6, 6"-H), 8.61 (s, 2H, terpyridine 3', 5'-H), 7.99-8.02 (t, J = 7.5 Hz, 2H, terpyridine 4, 4"-H), 7.80 (d, J = 7.5 Hz, 2H, phenyl H), 7.49 (m, 2H, terpyridine 5, 5"-H), 6.80 (d, J = 7.5 Hz, 2H, phenyl H), 4.59 (br, 1H, 12-OH), 3.95 (br, 1H, 3-OH), 3.85 (br, 1H, 12β-CH), 3.53 (br, 1H, 3β-CH), 3.25-3.50 (m, 4H, phenyl-NH-CH_2-CH_2), 0.80-2.35 (m, 27H, steroidal skeleton and alkyl H), 0.77 (s, 3H, 19-CH_3), 0.52 (s, 3H, 18-CH_3). ^{13}C NMR (125 MHz, $CDCl_3$): δ = 175.02, 156.57, 155.65, 149.88, 149.38, 149.03, 136.99, 128.35, 126.38, 123.76, 121.54, 117.57, 112.72, 73.09, 71.76, 48.04, 46.55, 46.47, 44.18, 42.05, 39.27, 36.49, 35.96, 35.21, 34.15, 33.65, 33.03, 31.45, 30.33, 29.72, 28.66, 27.60, 27.14, 26.06, 23.72, 23.17, 17.45, 12.65. HRMS (ESI), m/z calcd for $[C_{47}H_{59}N_5O_3\text{+H}]^+$ = 742.4696, found 742.4690.

Lithocholic acid-terpyridine conjugate (LCAtpy): ^{1}H NMR (500 MHz, $CDCl_3$): δ = 8.73 (d, J = 4.0 Hz, 2H, terpyridine 3, 3"-H), 8.69 (s, 2H, terpyridine 3', 5'-H), 8.66 (d, J = 8.0 Hz, 2H, terpyridine 6, 6"-H), 7.85-7.89 (t×d, J_1 = 7.5 Hz, J_2 = 2.0 Hz, 2H, terpyridine 4, 4"-H), 7.83 (d, J = 8.5 Hz, 2H, phenyl H), 7.34 (m, 2H, terpyridine 5, 5"-H), 6.72 (d, J = 8.5 Hz, 2H, phenyl H), 5.78 (m, 1H, CO*NH*), 4.41 (m, 1H, phenyl-*NH*), 3.63 (m, 1H, 3β-CH), 3.57 (m, 2H, phenyl-NH-CH_2), 3.56 (m, 2H, CO*NH*), 0.93-2.35 (m, 24H, steroidal skeleton and alkyl H), 0.91 (d, J = 6.5 Hz, 3H, 21-CH_3), 0.88 (s, 3H, 19-CH_3), 0.60 (s, 3H, 18-CH_3). ^{13}C NMR (125 MHz, $CDCl_3$): δ = 174.73, 156.63, 155.72, 149.92, 149.11, 149.05, 136.82, 128.35, 126.86, 123.65, 121.41, 117.57, 112.75, 71.85, 56.43, 55.90, 44.34, 42.73, 42.10, 40.41, 40.16, 39.22, 36.51, 35.82, 35.46, 35.36, 34.56, 33.53, 31.70, 30.54, 28.28, 27.18, 26.35, 24.19, 23.35, 20.80, 18.40, 12.00. HRMS (ESI), m/z calcd for $[C_{47}H_{59}N_5O_2\text{+H}]^+$ = 726.4747, found 726.4741.

Hexanoic acid-terpyridine conjugate (HAtpy): ^{1}H NMR (500 MHz, $CDCl_3$): δ = 8.72 (d, J = 4.0 Hz, 2H, terpyridine 3, 3"-H), 8.67 (s, 2H, terpyridine 3', 5'-H), 8.65 (d, J = 8.0 Hz, 2H, terpyridine 6, 6"-H), 7.84-7.88 (t×d, J_1 = 7.0 Hz, J_2 = 1.5 Hz, 2H, terpyridine 4, 4"-H), 7.78 (d, J = 8.5 Hz, 2H, phenyl H), 7.34 (m, 2H, terpyridine 5, 5"-H), 6.68 (d, J = 8.5 Hz, 2H, phenyl H), 6.03 (m, 1H, CO*NH*), 4.48 (br, 1H, phenyl-*NH*), 3.51 (m, 2H, phenyl-NH-CH_2), 3.30 (m, 2H, CO*NH*), 2.15 (t, J = 7.5 Hz, 2H, CH_2CO), 1.61 (m, 2H, alkyl CH_2), 1.23-1.34 (m, 4H, alkyl CH_2), 0.86 ((t, J = 8.0 Hz, 3H, -CH_3). ^{13}C NMR (125 MHz, $CDCl_3$): δ = 174.36, 156.58, 155.72, 149.97, 149.06, 136.87, 128.32, 126.76, 123.71, 121.42, 117.53, 115.25, 112.74, 44.28, 39.04, 36.68, 31.46, 25.39, 22.41, 13.95. HRMS (ESI), m/z calcd for $[C_{29}H_{31}N_5O\text{+H}]^+$ = 466.2606, found 466.2601.

2.5 Fluorescence quantum yield determination

The relative quantum yields (ϕ) of bile acid-terpyridine conjugates were determined by using quinine sulfate dehydrate dissolved in 0.1 M H_2SO_4 (ϕ= 54% at 350 nm) as a reference according to the following equation:[48]

$$\phi_c = \phi_{ref} \times (I_c / I_{ref}) \times (A_{ref} / A_c) (\eta_c / \eta_{ref})^2$$

where ϕ is the fluorescence quantum yield, I represents the measured integrated fluorescence intensity, and A denotes the optical intensity, and η is the refractive index of the solution. The subscript "*c*" and "*ref*" refer to the tested conjugates and reference fluorophore of known quantum yield. To minimize the reabsorption effects, the absorbencies of all the samples in 10 mm cuvette were kept under 0.1 at the excitation wavelength (360 nm).

2.6 Metal tunable optical studies

The optical response was performed at 25 ^{o}C by dissolving CAtpy, DCAtpy, or LCAtpy (3×10^{-4} M) in MeOH/H_2O (1/4, v/v) and adding a 1.5×10^{-4} M solution of metal ions in H_2O. The metal ions and bile acid conjugates were fully complexed for 2 h, then UV-Vis and fluorescence spectra were recorded. The chosen metal ions were $Cu(ClO_4)_2{\cdot}6H_2O$, $Mg(ClO_4)_2$, $Co(ClO_4)_2{\cdot}6H_2O$, $Cd(ClO_4)_2{\cdot}6H_2O$, $Mn(ClO_4)_2{\cdot}6H_2O$, $Al(ClO_4)_3{\cdot}9H_2O$,

$Zn(ClO_4)_2·6H_2O$, $Ni(ClO_4)_2·6H_2O$, $Tb(NO_3)_3·6H_2O$, $Eu(NO_3)_3·6H_2O$, $Fe(BF_4)_2·6H_2O$, $NaClO_4$, $CaCl_2$, $PdCl_2$. All emission spectra were recorded in the range of 390-700 nm after excitation at 360 nm. The slit size for excitation and emission wavelengths was 10 nm and a sealed quartz cuvette with a path length of a 1 cm was used.

2.7 Supramolecular self-assembly

CAtpy, DCAtpy, or LCAtpy (1 mg/mL) were dissolved in MeOH. Then the poor solvent H_2O was added dropwise under ultrasonic radiation until the appearance of Tyndall effect. The self-assembly of metal complexes adopted the similar approach. 5 μL of the sample was dropped on the copper mesh, let stand for 3-5 minutes, and the filter paper was used to absorb excess solvent to obtain a TEM sample.

3. Results and discussion

3.1 Synthesis

Scheme 1 displays the detailed synthetic routes of bile acid-terpyridine conjugates and the reference compound for control experiment. The bromophenyl substituted terpyridine was obtained by the reaction of 4-bromobenzaldehyde and 2-acetylpyridine in the presence of NaOH and concentrated NH_4OH in methanol. This intermediate was then treated with ethylenediamine in the presence of the catalyst CuCl, which resulted in the coupling reaction of the bromophenyl group with the amino group with relatively high yield (95%). Bile acid-terpyridine conjugates and the reference compound were obtained in one step amidation under a benign reaction condition. The intermediates and final products were fully characterized by ^1H, ^{13}C NMR, as well as mass spectroscopy and satisfactory results were obtained. All the bile acid-terpyridine conjugates can be dissolved in MeOH, CH_2Cl_2, THF, DMF and are completely insoluble in water.

3.2 Optical properties

Terpyridine and its derivatives represent a class of important ligands with good luminescence properties. Therefore, the absorbance and fluorescence spectra of bile acid-terpyridine conjugates were firstly investigated in the above mentioned solvents with the concentration of 5×10^{-5} M. As shown in Fig. 1a, the UV-Vis spectra of CAtpy display two absorption bands between 280 and 350 nm in the tested solvents. The absorption band at around 290 nm, which may be assigned to π-π* transition of terpyridine unit, don't show distinct difference in different polar solvents. While the band at longer wavelength, which may be ascribed to the intramolecular charge transfer (ICT) with ethylamino group as donor and terpyridine as acceptor, display apparent solvatochromism with changes in solvent polarity.[49] And the absorption peaks are observed at 333, 343, 343, and 348 nm in CH_2Cl_2, THF, MeOH, and DMF respectively (Fig. 1a, Table S1). For DCAtpy and LCAtpy, the similar absorption bands are obtained (Fig. 1b-1c, Table S2-S3). Upon excitation at 350 nm, the fluorescence spectra of CAtpy display strong emission at 450 nm and 458 nm in THF and CH_2Cl_2 respectively (Fig. 2a, Table S1). With increasing the solvent polarity, the fluorescence spectra exhibit red-shifted by ca. 50 nm to 503 nm in

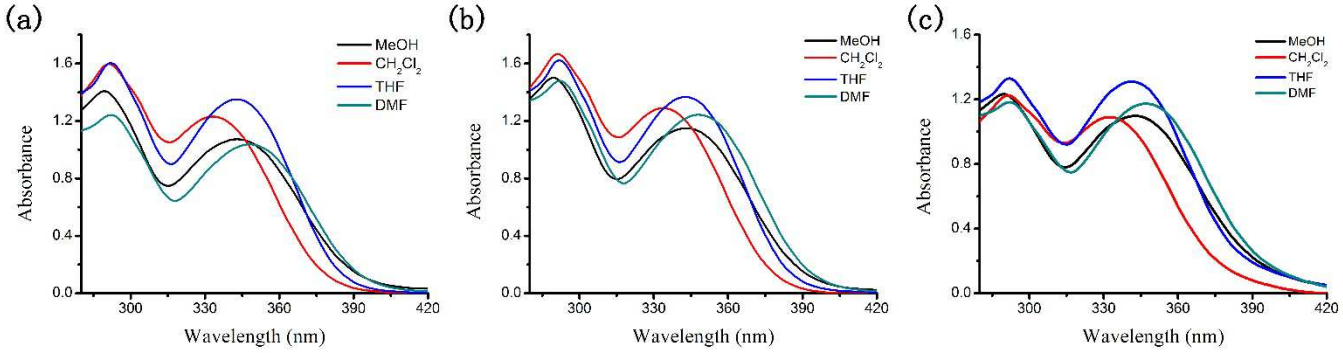

Fig. 1 UV-Vis spectra of CAtpy (a), DCAtpy (b) and LCAtpy (c) in different solvents.

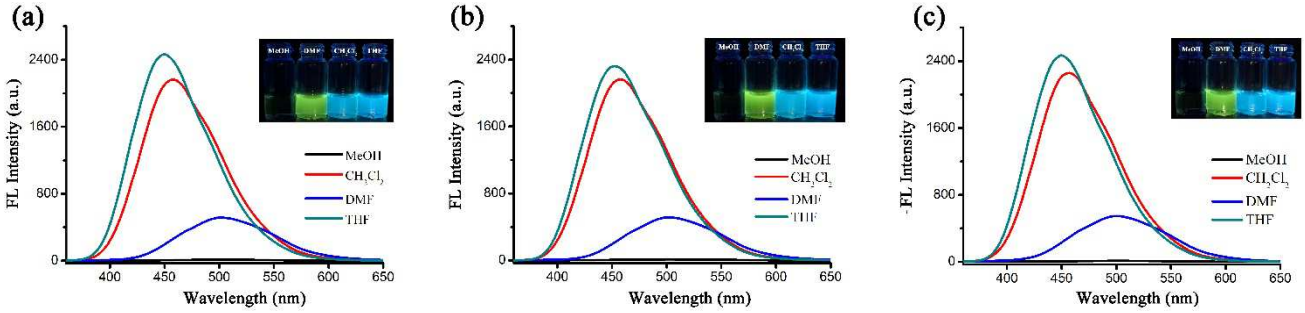

Fig. 2 Fluorescence spectra of CAtpy (a), DCAtpy (b) and LCAtpy (c) in different solvents; Insets: photographs taken under 365 nm UV illumination.

DMF (Fig. 2a, Table S1). As in the polar protic solvent MeOH, the fluorescence intensity of CAtpy dramatically decreases (Fig. 2a). Photographs of CAtpy solutions taken under 365 nm UV illumination show bright blue emission in THF and CH_2Cl_2, green emission in DMF and non-luminous in MeOH (Fig. 2a inset). The quantum yield of CAtpy are 33.50%, 15.80%, 15.75%, and 0.19% in CH_2Cl_2, THF, DMF and MeOH respectively (Table S1), which are in accordance with the fluorescence spectra of CAtpy. The distinguished difference of the emission phenomenon may be attributed to the twisted intramolecular charge transfer (TICT) state with a strong dependence on the solvent polarity.[50] It is worth noting that the fluorescence emission of CAtpy in MeOH is obviously quenched, which may be originated from the nonradiative decay of the rapid rotation of the phenyl rings connected to the terpyridine moiety.[14] For DCAtpy and LCAtpy, the similar emission spectra, luminescent photographs and quantum yields to CAtpy are observed (Fig. 2b-2c, Table S2-S3). The similarity of the optical properties of the three bile acid-terpyridine conjugates demonstrates that the steroidal skeletons with different amphiphilicity have no obvious effect on the luminescent property of terpyridine unit. The two fragments can retain their respective unique properties.

3.3 Aggregation - induced emission (AIE)

It is demonstrated that THF and MeOH are all good solvents for bile acid-terpyridine conjugates and the solution of three conjugates displayed distinctly different fluorescence phenomenon. So the polar protic and aprotic solvents are selected as the good solvents and water is used as poor solvent to study their AIE properties. Fluorescence spectra of the conjugates in THF-H_2O mixtures by varying water percentage were firstly examined. All the three conjugates exhibit strong blue light emission at about 450 nm in dilute THF solution (Fig. 3a-3c). Whereas the fluorescence intensity decreases sharply with the addition of water and the emission almost quenches with the water fraction (f_w) up to 10% for all the conjugates. Obviously, all the three bile acid-terpyridine conjugates exhibit quenching effect in THF-H_2O mixed solvents.

Then the AIE properties of three conjugates were further studied in MeOH-H_2O mixed solvents. As shown in Fig. S1-S3, increasing the water contents from 0% to 99%, the absorption spectra exhibit red shifts from 343 nm, 341 nm, and 341 nm to 355 nm, 361 nm and 354 nm for CAtpy, DCAtpy and LCAtpy, respectively. The fluorescence spectra hardly change with the increasing of water amount to 50%. The solutes are keeping clear with no aggregates formation. As continuing increasing the water content to 80%, the fluorescence intensities of three bile acid-terpyridine conjugates drastically increase to maximum values with slightly blue shift. The fluorescence intensity of CAtpy, DCAtpy and LCAtpy increase by 13-fold, 30-fold, 26-fold, respectively (Fig. 4). Correspondingly, the quantum yields of CAtpy, DCAtpy and LCAtpy also rise by 2-fold, 21-fold, 19-fold respectively at f_w = 80% (Table S1-S3). Photographs of the three conjugates solutions taken under 365 nm UV illumination also show the distinct AIE phenomenon after increasing the water content to 50% (Fig. 5). Furthermore, the fluorescence intensity of the three derivatives decreases when the water fraction is more than 80% (Fig. 4 insets), which is probably due to the quick agglomeration of the conjugates in a random way and forms less emissive amorphous powders.[51]

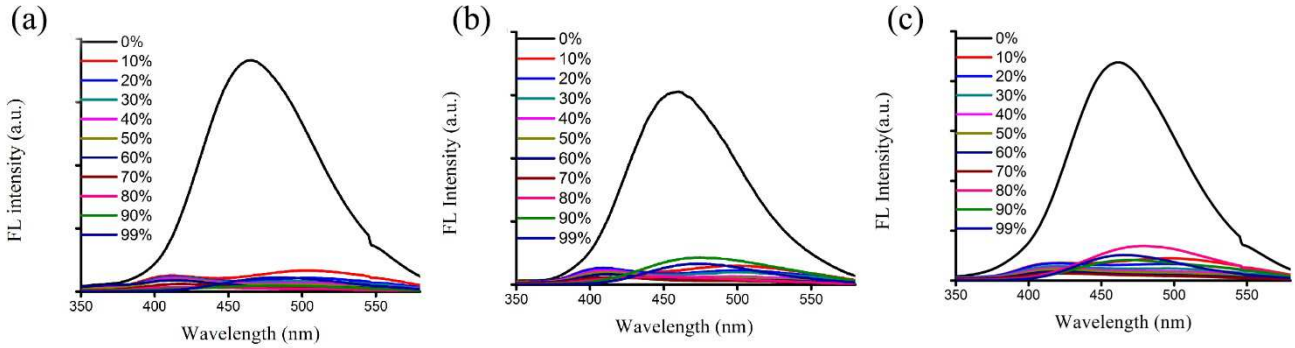

Fig. 3 Fluorescence spectra of CAtpy (a), DCAtpy (b) and LCAtpy (c) in THF-H_2O mixtures with different H_2O contents.

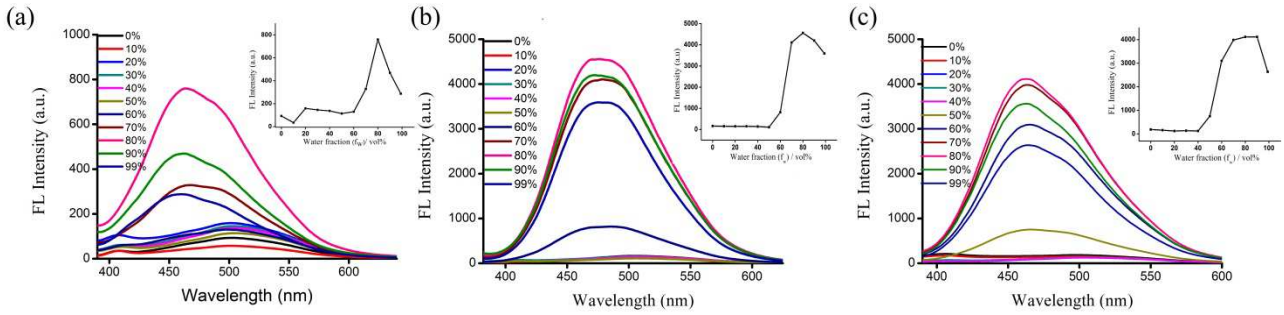

Fig. 4 Fluorescence spectra of CAtpy (a), DCAtpy (b) and LCAtpy (c) in MeOH-H_2O mixtures with different H_2O contents.

Obviously, the three bile acid-terpyridine conjugates exhibit typical AIE properties in MeOH-H_2O mixed solvents. This may be attributed to the formation of nano-sized particles and the resulted restriction of intramolecular rotations (RIR) of the terpyridine rings in the aggregates enhance light emission.[52-54] The formed aggregates at f_w = 80% were examined by transmission electron microscopic (TEM), which showed that CAtpy, DCAtpy and LCAtpy had spherical structures with diameters of around 400-500 nm (Fig. 6). It is noteworthy that terpyridine and its derivatives represent a class of important metal chelating ligands with weakly luminescent ($\phi_{em} = 3 \times 10^{-3}$). They are not typical traditional AIE active luminogens. Although some studies dealing with metal-terpyridine complexes with AIE properties as chemosensors,[23, 25, 29, 31] only a few examples of terpyridine and its derivatives as active AIE luminogens have been reported in the literature.[24, 27, 28] Bile acids are a class of natural occurring compounds with rigid steroidal skeleton and unique facial amphiphilicity. They can be excellent building blocks in supramolecular chemistry and can be designed as a variety of functional chemical systems.[55-57] It is a pity that they possess no luminescence properties. The AIE origin of bile acid-terpyridine conjugates stimulated our great interests.

By carefully observing the AIE phenomenon in MeOH-H_2O mixed solvents, it is found that the fluorescence intensity begins to enhance at different water contents for CAtpy, DCAtpy and LCAtpy. As shown in Scheme 1, the difference between CAtpy, DCAtpy and LCAtpy is the structure of bile acid skeleton connected to terpyridine unit. And the difference between CA, DCA and LCA is the number of hydroxyl group on steroidal skeleton, which decreases gradually and leads to the difference of amphiphilicity and self-assembly phenomenon of CA, DCA and LCA. Consequently, CAtpy, DCAtpy and LCAtpy exhibit different properties, resulting in the difference of AIE phenomenon. As shown by Fig. 4, the fluorescence intensity of CAtpy, DCAtpy, and LCAtpy begin to increase from f_w = 60%, 50%, and 40%, respectively. It is anticipated that the bile acid skeleton with excellent assembly properties can restrict the rotation of terpyridine unit thus resulting in the enhancement and difference of AIE properties.

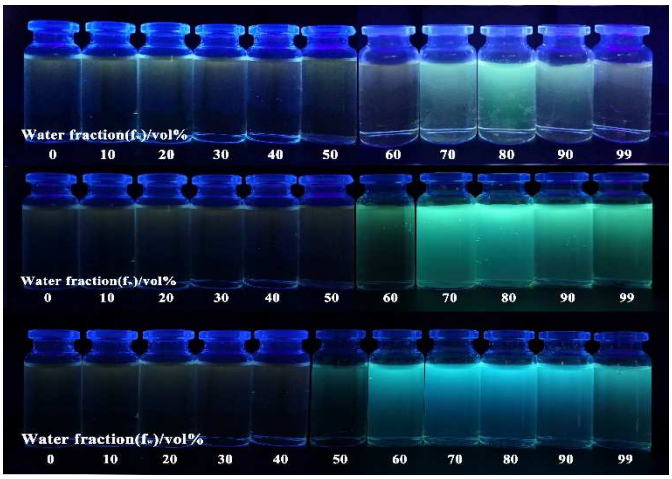

Fig. 5 Photographs of CAtpy (a), DCAtpy (b) and LCAtpy (c) in MeOH-H_2O mixtures with different H_2O contents taken under 365 nm UV illumination.

In order to further investigate whether bile acid skeleton plays a key role in the generation of the AIE phenomenon, a linear hexanoic acid-terpyridine (HAtpy) conjugate as a reference compound was synthesised and the AIE properties were thoroughly investigated. As shown in Fig. 7, the fluorescence intensity of HAtpy in MeOH (at c.a. 502 nm) is very weak and the photograph under 365 nm shows no obvious emission (Fig. 8). As increasing the water content to 80%, the emission intensity begins to increase and reaches maximum value at f_w = 99% with about 2-fold enhancement, which is in accordance with the photographs under 365 nm UV illumination (Fig. 8). It is revealed that HAtpy in MeOH-H_2O also exhibits AIE properties. However, the enhancement of fluorescence intensity is much lower than that of bile acid-terpyridine conjugates, further indicating that the AIE phenomenon originates from the terpyridine unit and the bile acid unit with rigid steroidal skeleton and self-assembly properties can strengthen the AIE intensity, while the flexible hexanoic acid chain has little effect on the AIE intensity.

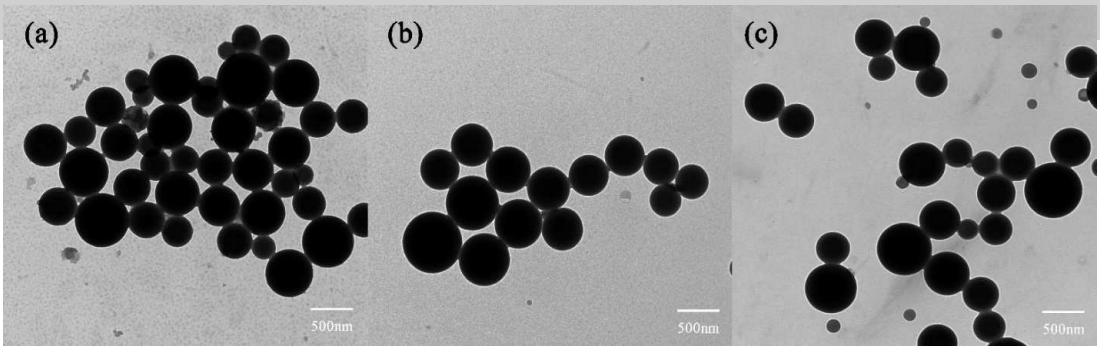

Fig. 6 TEM images of CAtpy (a), DCAtpy (b) and LCAtpy (c) in MeOH-H_2O mixed solvents.

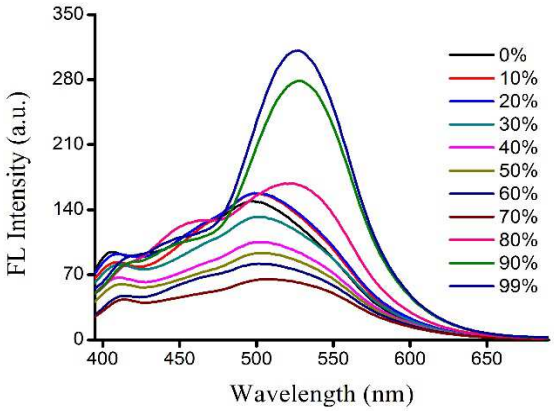

Fig. 7 Fluorescence spectra of HAtpy in MeOH-H_2O mixtures with different H_2O contents.

Fig. 8 Photographs of HAtpy in MeOH-H_2O mixtures with different H_2O contents taken under 365 nm UV illumination.

3.4 Optical response to metal ions

Terpyridine and its derivatives represent a class of important metal chelating unit. The response of the AIE aggregates of bile acid-terpyridine conjugates to different metal ions was further studied. The experiments were carried out using their nanoaggregates in MeOH-water mixture (1/4, v/v), which showed intensified fluorescence emission properties. Fig. 10 shows the fluorescence response of the nanoaggregates to various metal ions. For CAtpy, in the presence of Na^+, Ca^{2+}, Mg^{2+}, Tb^{3+} and Eu^{3+} cations, the spectral patterns keep unchanged with the fluorescence intensity becomes weaker or slightly stronger. The corresponding emission colours under 365 nm are still blue-green without obvious change (Fig. 9). Al^{3+}, Mn^{2+} and Pd^{2+} ions make the emission intensity decrease significantly. Cu^{2+} and group VIIIB metal cations (Fe^{3+}, Co^{2+}, Ni^{2+}) efficiently quench the emission of CAtpy. Whereas, the addition of Zn^{2+} and Cd^{2+} to CAtpy aggregates causes the emission spectra to shift to the longer wavelengths with only weak fluorescence[58] (Fig. 10a, 10d). The emission colour changes from bluish-green to yellow (Fig. 9a). It is conjectured that complexing with Zn^{2+} and Cd^{2+} can strengthen the electron-withdrawing ability of terpyridine and thus promotes the occurrence of the ICT process from the amino group to the terpyridine-Zn^{2+} moiety, thereby making the emission shift to the longer wavelength. The reduction of fluorescence intensity induced by Zn^{2+} and Cd^{2+} binding is often observed when the terpyridine unit is connected to the π-conjugated part. For DCAtpy and LCAtpy, the similar emission spectra and colour change are observed. The changes in the fluorescence intensity and the emission maximum (λ_{max}) with various metal ions in MeOH-H_2O mixture (1/4, v/v) are summarized in Table S1-

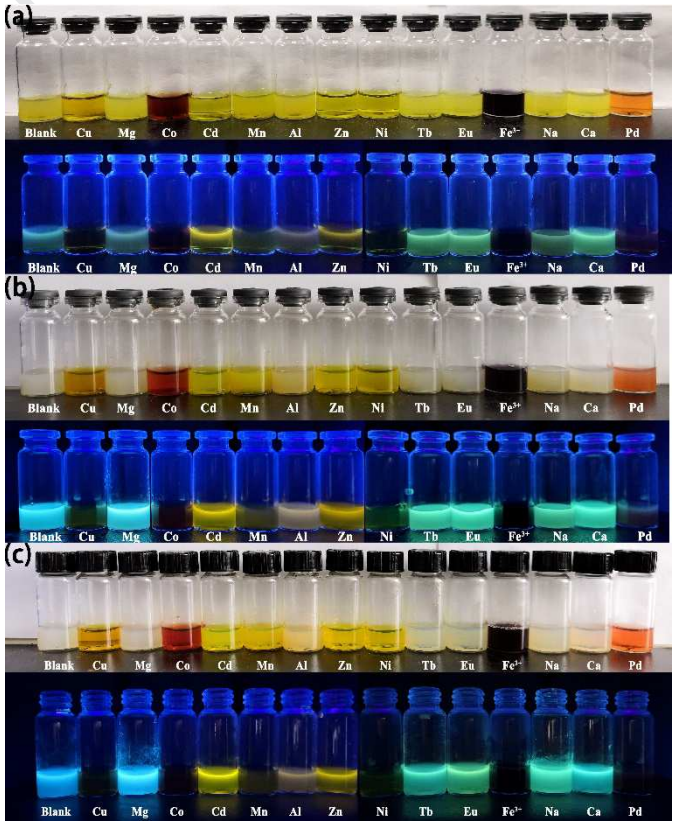

Fig. 9 Photographs of MeOH-water mixtures (1/4, v/v) of (a) CAtpy/cation, (b) DCAtpy/cation and (c) LCAtpy/cation mixtures taken under 365 nm UV illumination.

S3. The λ_{max} values of CAtpy, DCAtpy and LCAtpy are red-shifted by ca. 90 nm, 82 nm, and 83 nm, respectively in the presence of Zn^{2+} ions. Cd^{2+} ions exert the similar bathochromic

shift under the same experimental conditions. The fluorophores also show yellow emission when complex with Zn^{2+} and Cd^{2+} cations (Fig. 9b-9c).

The remarkable fluorescence and colour changes brought by Zn^{2+} and Cd^{2+} stimulate our interest to further investigate the properties of Zn^{2+} and Cd^{2+} complexes. Because CAtpy, DCAtpy and LCAtpy exhibit similar response behaviour to Zn^{2+} and Cd^{2+} cations, we will focus our discussion on the metal response property of CAtpy in the following investigation. Upon addition of Zn^{2+} to CAtpy in a mixed solvent of MeOH and H_2O (1/4, v/v) as shown in Fig. S4a, the increase in the absorption peak at 420 nm is observed, while the band at 355 nm decreases, with the isosbestic point at 380 nm. The enhancement of absorption maximum at 420 nm is ascribed to CAtpy and Zn^{2+} coordinative interactions. The fluorescence titration of CAtpy with Zn^{2+} shows a gradual decrease in the emission intensity with 90 nm red shift of the emission maxima (Fig. S6a, 463 nm to 553 nm) and change in the emission spectra rapidly leveled off after addition of 0.5 equivalent of Zn^{2+} ions (Fig S6d). The fluorescence quantum yield slightly decreases (ϕ = 0.30% to 0.21%) upon Zn^{2+} addition. The emission intensity also shows plateau with more than 0.5 equivalent of Zn^{2+}. The coordination behaviour of CAtpy with Zn^{2+} is also confirmed using ^1H NMR spectra. Upon addition of 0.5 equivalent of Zn^{2+}, the signals of terpyridine unit shift to downfield (Fig. S8). These facts obviously indicate that the formation of CAtpy-Zn^{2+} complex with a ratio of 2:1. The absorption and fluorescence titration of CAtpy with Cd^{2+}, DCAtpy and LCAtpy with Zn^{2+} and Cd^{2+} show similar results with a little difference in the intensity of absorption and emission maxima , as shown in Fig. S4-S7.

The above results indicate that CAtpy, DCAtpy and LCAtpy display the similar response to various metal ions and various colourful metal complexes are obtained. The difference in the steroidal skeleton cannot affect the metal response of terpyridine unit.

3.5 Regulation of supramolecular morphology by metal ions

Bile acid with rigid steroidal skeleton and amphiphilic molecular structure exhibits excellent self-assembly properties. A series of attractive morphologies, including nanocapsules, twisted ribbons, nanotubes, nanofibers and wrinkle structures *etc.* were constructed by bile acid derivatives. Thus, we further investigated the supramolecular morphology of bile acid-terpyridine conjugates in MeOH-H_2O mixture with or without metal ions. As shown in Fig. 6a-c, spherical aggregates with average size around 400-500 nm are obtained for CAtpy, DCAtpy and LCAtpy. The complexation with Zn^{2+} and Cd^{2+} ions cannot alter the morphology of CAtpy, DCAtpy and LCAtpy, but exhibit excellent size tunability. Smaller spherical aggregates of average size 100-200 nm are obtained (Fig. 11, S9).

4. Conclusions

In summary, a series of bile acid-terpyridine conjugates were synthesized through simple amidation reaction. The bile acid skeleton with unique rigid skeleton and amiphiphilicity can tune the AIE properties of terpyridine units, making the three conjugates exhibiting distinct AIE phenomenon in MeOH-H_2O solvents. Furthermore, with the metal chelating terpyridine units, the optical properties of the AIE bile acid-terpyridine conjugates can be tuned by different metal ions leading to colourful complexes. Especially by combining Zn^{2+} and Cd^{2+} ions, the emission maxima can red shift by 90 nm, resulting in the complexes with yellow light emission. The self-assembly property of amphiphilic bile acid skeleton can tune the terpyridine units to form spherical aggregates in MeOH-H_2O solvents. And the self-assembly morphology size can be well-tuned by the complexation of metal ions. These biological conjugates with controllable AIE properties and metal tunable fluorescence and supramolecular assembly properties may provide a new avenue for the bioimaging and drug controllable delivery system.

Acknowledgements

We gratefully acknowledge the financial support from the National Science Foundation of China (21403122) and High-level Science Foundation of Qingdao Agricultural University (6631405). We thank Dr. Fengying Dong of Central Laboratory of QAU for the NMR test and Dr. Jing Liu of Central Laboratory of QAU for the TEM test.

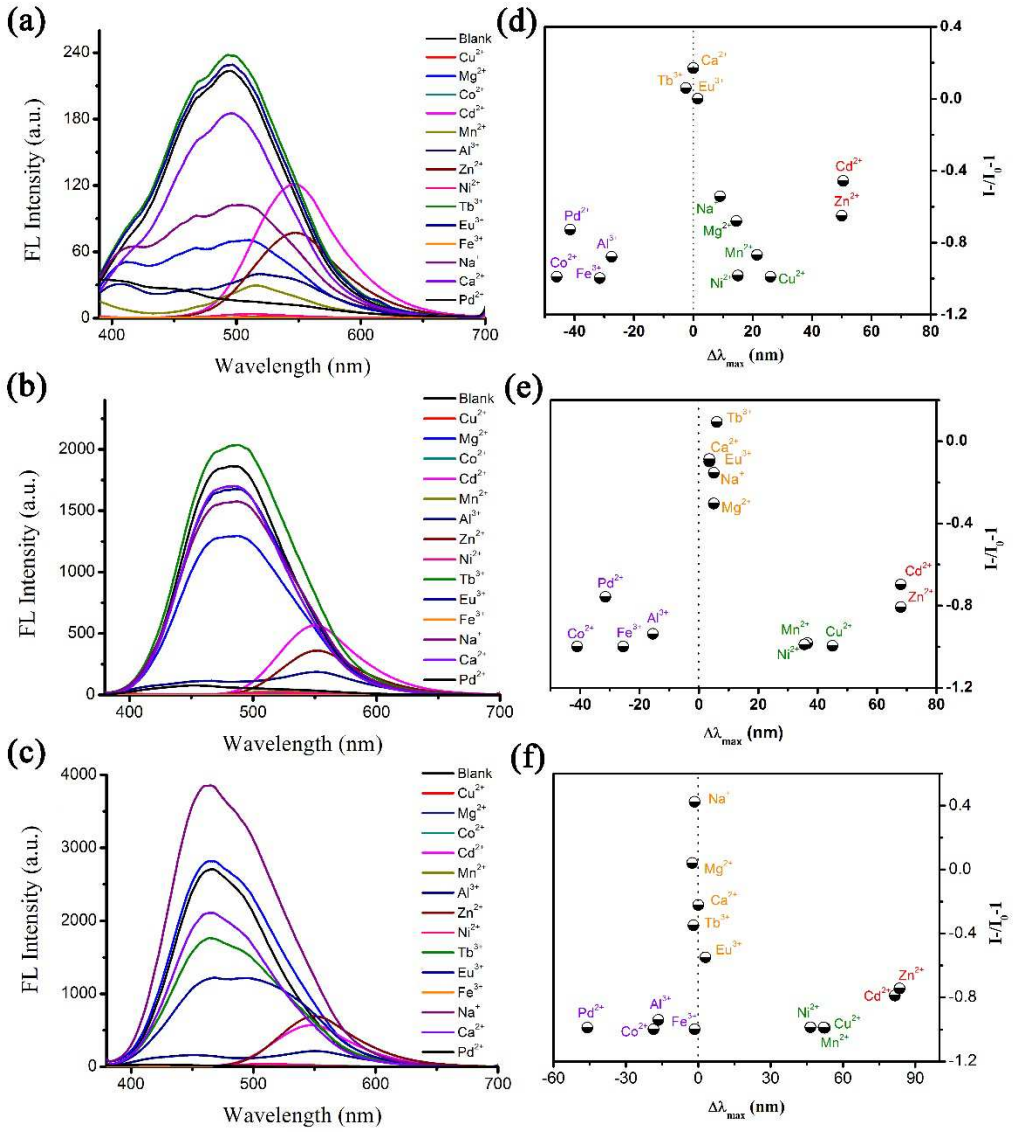

Fig. 10 Fluorescence spectra of CAtpy (a), DCAtpy (b) and LCAtpy (c) in the presence of various cations in MeOH-water mixtures (1/4, v/v). Fluorescence response of nanoaggregates of CAtpy (d), DCAtpy (e) and LCAtpy (f) to cations. The x-axis and y-axis corresponds to the shift in the emission maximum (λ_{max}) and the enhancement of fluorescence intensity as referred to the fluorescence spectra without metal ions.

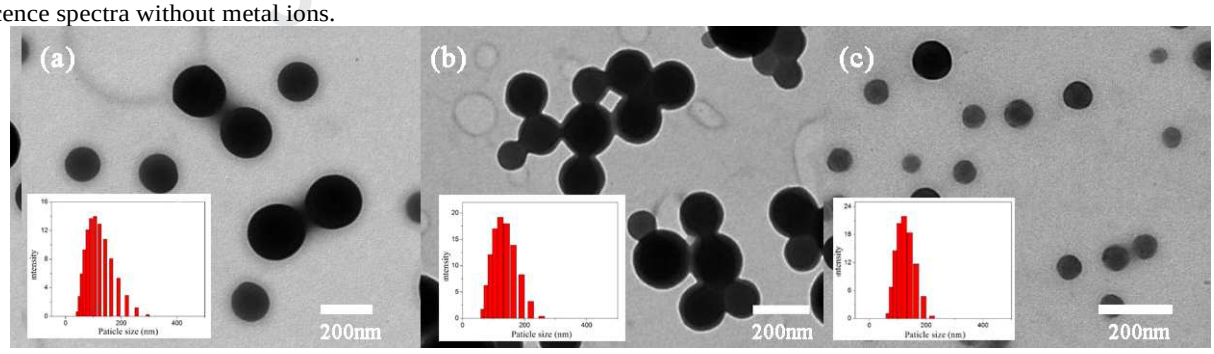

Fig. 11 Particle size distributions of CAtpyZn (a), DCAtpyZn (b) and LCAtpyZn (c) in MeOH-H_2O mixtures (1/4, v/v).

Notes and references

1. H. J. Jin, H. P. Li, Z. Y. Zhu, J. B. Huang, Y. L. Xiao and Y. Yan, *Angew. Chem. Int. Ed.*, DOI: 10.1002/anie.201911845.
2. I. Yildiz, E. Deniz and F. M. Raymo, *Chem. Soc. Rev.*, 2009, **38**, 1859-1867.
3. M. Pan, W. M. Liao, S. Y. Yin, S. S. Sun and C. Y. Su, *Chem. Rev.*, 2018, **118**, 8889-8935.
4. C. Fan and C. L. Yang, *Chem. Soc. Rev.*, 2014, **43**, 6439-6469.
5. W. Y. Wong and C. L. Ho, *J. Mater. Chem.*, 2009, **19**, 4457-4482.
6. E. Holder, N. Tessler and A. L. Rogach, *J. Mater. Chem.*, 2008, **18**, 1064-1078.
7. J. C. Li and K. Y. Pu, *Chem. Soc. Rev.*, 2019, **48**, 38-71.
8. F. Hu, S. D. Xu and B. Liu, *Adv. Mater.*, 2018, **30**, 1801350.

9. S. J. Chen, H. Wang, Y. N. Hong and B. Z. Tang, *Mater. Horiz.*, 2016, **3**, 283-293.
10. S. V. Eliseeva and J. C. G. Bunzli, *Chem. Soc. Rev.*, 2010, **39**, 189-227.
11. X. G. Hou, Y. Wu, H. T. Cao, H. Z. Sun, H. B. Li, G. G. Shan and Z. M. Su, *Chem. Commun.*, 2014, **50**, 6031-6034.
12. J. D. Luo, Z. L. Xie, J. W. Y. Lam, L. Cheng, H. Y. Chen, C. F. Qiu, H. S. Kwok, X. W. Zhan, Y. Q. Liu, D. B. Zhu and B. Z. Tang, *Chem. Commun.*, 2001, 1740-1741.
13. B. Z. Tang, X. W. Zhan, G. Yu, P. P. S. Lee, Y. Q. Liu and D. B. Zhu, *J. Mater. Chem.*, 2001, **11**, 2974-2978.
14. H. Tong, Y. Hong, Y. Dong, M. Haussler, J. W. Y. Lam, Z. Li, Z. F. Guo, Z. H. Guo and B. Z. Tang, *Chem. Commun.*, 2006, 3705-3707.
15. Q. Zeng, Z. Li, Y. Dong, C. Di, A. Qin, Y. Hong, L. Ji, Z. Zhu, C. K. W. Jim, G. Yu, Q. Li, Z. Li, Y. Liu, J. Qin and B. Z. Tang, *Chem. Commun.*, 2007, 70-72.
16. M. Chen, L. Z. Li, H. Nie, J. Q. Tong, L. L. Yan, B. Xu, J. Z. Sun, W. J. Tian, Z. J. Zhao, A. J. Qin and B. Z. Tang, *Chem. Sci.*, 2015, ***6***, 1932-1937.
17. J. W. Chen, B. Xu, X. Y. Ouyang, B. Z. Tang and Y. Cao, *J. Phys. Chem. A*, 2004, **108**, 7522-7526.
18. Y. N. Hong, J. W. Y. Lam and B. Z. Tang, *Chem. Soc. Rev.*, 2011, **40**, 5361-5388.
19. E. C. Constable, *Chem. Soc. Rev.*, 2007, **36**, 246-253.
20. H. Hofmeier and U. S. Schubert, *Chem. Soc. Rev.*, 2004, **33**, 373-399.
21. G. F. Swiegers and T. J. Malefetse, *Chem. Rev.*, 2000, **100**, 3483-3537.
22. A. Wild, A. Winter, F. Schlutter and U. S. Schubert, *Chem. Soc. Rev.*, 2011, **40**, 1459-1511.
23. S. H. Jung, K. Y. Kwon and J. H. Jung, *Chem. Commun.*, 2015, **51**, 952-955.
24. V. D. Singh, B. K. Dwivedi, R. P. Paitandi, Y. Kumar and D. S. Pandey, *Inorg. Chim. Acta*, 2019, **487**, 24-30.
25. D. B. Chao and S. T. Ni, *Sci. Rep.*, 2016, **6**, 26477.
26. Y. Li, Z. Y. Gu, T. He, X. C. Yuan, Y. Y. Zhang, Z. Xu, H. Y. Qiu, Q. Zhang and S. C. Yin, *Dyes Pigments*, 2020, **173**, 107969.
27. C. K. Zhang, Y. Q. Zhao, D. D. Li, J. J. Liu, H. G. Han, D. Y. He, X. H. Tian, S. L. Li, J. Y. Wu and Y. P. Tian, *Chem. Commun.*, 2019, **55**, 1450-1453.
28. J. B. Guo, X. D. Yu, Z. Zhang and Y. J. Li, *J. Colloid Interf. Sci.*, 2019, **540**, 134-141.
29. V. D. Singh, R. P. Paitandi, B. K. Dwivedi, R. S. Singh and D. S. Pandey, *Organometallics*, 2018, **37**, 3827-3838.
30. Z. Zhou, F. L. Gu, L. Peng, Y. Hu and Q. M. Wang, *Chem. Commun.*, 2015, **51**, 12060-12063.
31. A. Fermi, G. Bergamini, M. Roy, M. Gingras and P. Ceroni, *J. Am. Chem. Soc.*, 2014, **136**, 6395-6400.
32. S. Mukhopadhyay and U. Maitra, *Curr. Sci. India*, 2004, **87**, 1666-1683.
33. Y. Zhao and Z. Q. Zhong, *J. Am. Chem. Soc.*, 2005, **127**, 17894-17901.
34. Y. Zhao and Z. Q. Zhong, *J. Am. Chem. Soc.*, 2006, **128**, 9988-9989.
35. Y. Zhao, Z. Q. Zhong and E. H. Ryu, *J. Am. Chem. Soc.*, 2007, **129**, 218-225.
36. S. S. Song, R. H. Dong, D. Wang, A. X. Song and J. C. Hao, *Soft Matter*, 2013, **9**, 4209-4218.
37. Y. Qiao, Y. Y. Lin, Y. J. Wang, Z. Y. Yang, J. Liu, J. Zhou, Y. Yan and J. B. Huang, *Nano Lett.*, 2009, **9**, 4500-4504.
38. X. J. Zhang and J. Y. Fang, *Soft Matter*, 2010, **6**, 2139-2142.
39. Y. Li, G. Li, X. Wang, C. Lin, Y. Zhang and Y. Ju, *Chem. Eur. J.*, 2008, **14**, 10331-10339.
40. Y. Li, G. T. Li, X. Y. Wang, W. N. Li, Z. X. Su, Y. H. Zhang and Y. Ju, *Chem. Eur. J.*, 2009, **15**, 6399-6407.
41. W. Li, T. Tian, Y. Lan, W. Zhu, J. Li, M. Zhang, Y. Ju and G. Li, *Polym. Chem.*, 2014, **5**, 743-751.
42. M. Zhang, X. P. Yin, T. Tian, Y. Liang, W. N. Li, Y. Lan, J. Li, M. M. Zhou, Y. Ju and G. T. Li, *Chem. Commun.*, 2015, **51**, 10210-10213.
43. J. Z. Sun, S. S. Xiang, X. Xu, W. N. Li and J. S. Shi, *Tetrahedron Lett.*, 2016, **57**, 2125-2128.
44. J. E. Gautrot and X. X. Zhu, *Macromolecules*, 2009, **42**, 7324-7331.
45. J. E. Gautrot and X. X. Zhu, *Angew. Chem. Int. Ed.*, 2006, **45**, 6872-6874.
46. Y. G. Jia, C. Malveau, M. A. Mezour, D. F. Perepichka and X. X. Zhu, *Angew. Chem. Int. Ed.*, 2016, **55**, 11979-11983.
47. O. Jurcek, P. Bonakdarzadeh, E. Kalenius, J. M. Linnanto, M. Groessl, R. Knochenmuss, J. A. Ihalainen and K. Rissanen, *Angew Chem Int Ed*, 2015, **54**, 15462-15467.
48. M. Grabolle, M. Spieles, V. Lesnyak, N. Gaponik, A. Eychmuller and U. Resch-Genger, *Anal. Chem.*, 2009, **81**, 6285-6294.
49. M. Kong, Y. Z. Zhu, W. Du, Q. Zhang, X. H. Tian, S. L. Li, H. P. Zhou, J. Y. Wu and Y. P. Tian, *Dyes Pigments*, 2018, **158**, 225-232.
50. P. Mahato, S. Saha and A. Das, *J. Phys. Chem. C*, 2012, **116**, 17448-17457.
51. X. Y. Shi, H. Wang, T. Y. Han, X. Feng, B. Tong, J. B. Shi, J. G. Zhi and Y. P. Dong, *J. Mater. Chem.*, 2012, **22**, 19296-19302.
52. V. D. Singh, R. P. Paitandi, B. K. Dwivedi, R. S. Singh and D. S. Pandey, *Organometallics*, 2018, **37**, 3827-3838.
53. Dong. Y, Shen. J, Li. W, Zhao. R, Pan. Y, Song. Q, Zhang. C. *Tetrahedron*, 2019, **75**, 2670-2675.
54. Kumar. V, Naik. V. G, Das. A, Basu Bal, S, Biswas. M, Kumar. N, Ganguly. A, Chatterjee. A, Banerjee. M. *Tetrahedron*, 2019, **75**, 3722-3732.
55. X. X. Zhu and M. Nichifor, *Acc. Chem. Res.*, 2002, **35**, 539-546.
56. A. P. Davis, *Molecules*, 2007, **12**, 2106-2122.
57. J. Zhang and X. Zhu, *Sci. China Ser. B*, 2009, **52**, 849-861.
58. B. N. Ghosh, F. Topic, P. K. Sahoo, P. Mal, J. Linnera, E. Kalenius, H. M. Tuononen and K. Rissanen, *Dalton Trans.*, 2015, **44**, 254-267.

1. A series of conjugates combining bile acid and terpyridine units were developed.
2. The aggregates of the conjugates can strongly confine and tune the rotation of terpyridine units to endow the conjugates with excellent AIE properties.
3. The conjugates exhibit excellent metal response properties and lead to various colourful complexes.
4. The supramolecular assembly morphology can be well controlled by the metal ions.

Statements

1. Submitter declares that all authors have seen and approved the submission of the manuscript, and the manuscript has been submitted exclusively to *Tetrahedron*.
2. All other related works from my laboratory that are currently under consideration for publication in this or other journals have been properly cited in the present manuscript, and that all related published works by my laboratory have been properly cited in this manuscript.
3. This manuscript is not under consideration for publication elsewhere and that no portion has been published elsewhere in any medium including electronic journals and computer databases of a public nature.
4. No portions of text or wording in the present manuscript have been duplicated from previous work published by me or by other authors.